Journal of Molecular Graphics and Modelling 29 (2010) 82–92

Contents lists available at ScienceDirect

Journal of Molecular Graphics and Modelling

journal homepage: www.elsevier.com/locate/JMGM

Conformational study of methylphosphocholine: a prototype for phospholipid headgroups in membranes

Cinthia S. Soares, Clarissa O. da Silva*

Departamento de Química, Universidade Federal Rural do Rio de Janeiro, BR 465, km 47, CEP 24949-900 Seropédica, Rio de Janeiro, Brazil

ARTICLE INFO

Article history:
Received 14 February 2010
Received in revised form 4 May 2010
Accepted 5 May 2010
Available online 12 May 2010

Keywords:
Phospholipid membrane
Methylphosphocholine
Membrane head conformation
Membrane description
Potential curves for MePC dihedral space

ABSTRACT

Phospholipid bilayers constitute the largest structural component of cell membranes, in which choline phospholipids are abundant. In this study, through a theoretical sampling on a methylphosphocholine (MePC) potential energy surface, a set of conformers was selected as a prototype for the membrane phospholipid head. We performed a detailed conformational study of such a prototype, both as an isolated moiety and in a solvated system. We used the polarizable continuum model (PCM) to account for solvation effects. We used a quantum-mechanical methodology based on density functional theory (DFT) and the 6-31G(d,p) basis set for the calculations. Through this methodology we were able to obtain a set of conformations that presented a mirror-image pattern, in good agreement with the experimental geometric values for the different phosphocholine derivatives. Potential curves for the main parameters of the dihedral space of MePC were obtained and are provided to guide future force-field parameterizations.

1. Introduction

Cell membranes are basically made of lipids and proteins [1]. Among the lipids present in cell membranes, the class of phospholipids stands out, with the subclass of choline phospholipids being the most abundant [2]. The chemical structure of membrane phospholipids is very special: one of its ends displays a hydrophilic feature while the other displays a hydrophobic feature. Due to these characteristics, it is possible for them to arrange themselves in bilayers, where the hydrophobic portions are in contact with each other. Because of this difference in chemical structure, these molecules are said to be amphipathic, and the hydrophilic portion is often called a phospholipid head. When organized into bilayers, the phospholipids are arranged in such a way that both faces display a hydrophilic feature, which is essential in intra- and extracellular aqueous environments.

The surfaces of cellular membranes are important sites, where many different exogenous substance–membrane interactions take place. Among these interactions, the trehalose–membrane interaction is noteworthy because it is intimately related to cellular viability in the processes of the preservation of tissues and microorganisms in the absence of water [3–6]. Clearly, such preservation is dependent on many other factors, the trehalose–membrane interaction being only one of them [7].

This interaction is far from fully understood, and at least three models (not necessarily mutually exclusive [8]) can be found in the literature to explain it: the water-replacement model, the water-enclosure model [9] and the glassy-state formation model [10]. For the latter, however, to the best of our knowledge, no microscopic description of the interactions responsible for it has been presented to date. Nevertheless, taking into account the findings of Grigera and Caffarena [11,12], we can say that in the glassy state the mobility of water molecules is much more restricted than in the rubbery state (for a glucose solution), the residence time of the sugar–water hydrogen bonds being greatly increased.

Molecular-dynamics studies have found that the trehalose–membrane interaction occurs mainly between the disaccharide (a polyhydroxylated compound) and the phospholipid headgroups of membranes [13–15]. This was concluded based on the observation of a higher local concentration of carbohydrates near the headgroup-region of the membrane as compared to the bulk. This has also been found in experimental works [16–18]. These theoretical works have begun to discuss the carbohydrate–membrane interaction mechanism in detail [13–15,19], and perhaps could be complemented by quantum-mechanical investigations of this very complex system, given the availability of reliable quantum-mechanical prototypes (the disaccharides have been studied elsewhere [20]). Although the membrane is a very complex system, it may be possible to quantify the local carbohydrate–phospholipid interaction through a quantum-mechanical description if the errors associated with the effects of the surroundings (neglected in the prototypes) are systematic to all disaccharides studied.

* Corresponding author. Tel.: +55 21 2682 2907; fax: +55 21 2682 2907.
E-mail address: clarissa-dq@ufrrj.br (C.O. da Silva).

1093-3263/$ – see front matter © 2010 Elsevier Inc. All rights reserved.
doi:10.1016/j.jmgm.2010.05.001

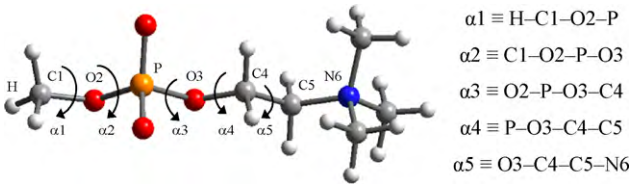

Fig. 1. The main dihedral angles defining the conformation of the phospholipid headgroups.

From our point of view, any theoretical study devoted to a better understanding of the structural and energetic properties of the phospholipid bilayers must encompass two different investigational stages: a conformational (and energetic) analysis of the phospholipid as a monomeric unit (divided into hydrophilic and hydrophobic parts) and a subsequent study of the possible structural and energetic changes that arise from the interaction of these monomers. Therefore, in the present study, we performed a conformational study of methylphosphocholine (MePC) because it is the most abundant headgroup in cellular membranes [2]. This Boltzmann statistical analysis was necessary because the active conformations (i.e., those able to interact with the cellular exogenous substances) can be found not only at the global minimum but also at any of the local minima if they have energy values very close to the global minimum at typical conditions.

The majority of theoretical studies performed to obtain information about the phospholipid bilayer have so far been conducted through classical molecular-dynamics simulations (MD) [21–30]. Until now, relatively few studies using quantum-mechanical methods have been performed to describe theoretical systems like this, and the electronic correlation effects have been neglected in almost all of them. Generally in these latter studies, structural data were obtained from pure crystals or from an analysis performed in systems in a liquid-crystalline or gel phase. Where the working structure was not rigid, all experimental information was obtained as mean values and represent average expressions of sets of coexisting conformations, and are thus a sometimes unreliable source of geometric information for quantum-mechanical studies.

Due to the large size of phospholipids, quantum-mechanical models (QM) devoted to studying the phospholipid bilayer have been restricted to exploring the properties of the phospholipid headgroups as an initial step towards characterizing the individual phospholipid units composing cell membranes. In 1974, Pullman and Berthod [31] performed one of the pioneering studies in the literature, where a QM methodology was employed to describe a membrane phospholipid fragment. In this study, the authors reported as suspicious the similarity between the geometric parameters obtained from crystallography and those found through NMR in solution for phosphoethanolamine (PE) (a fact confirmed in the 1990s by Bruzik and Harwood [32] and more recently by Aussenac et al. [33]). The authors disagreed with the idea that the conformations obtained in the solid phase and in solution were the same because very different intrinsic stabilization effects defined each one. In their study, using a Hartree–Fock methodology (HF) and an STO-3G basis set, the authors calculated a potential energy surface (PES) for phosphoethanolamine (PE), where the α4 and α5 geometrical parameters were changed (see Fig. 1), assuming as the starting conformations those conformations with the geometric parameters obtained by crystallography. They found a conformation with α4 = 300° and α5 = 90° as the global minimum in the gas phase, a finding that was different from those experimentally reported (α4 ≈ 180° and α5 = 60° or 300°). They concluded that these were not the intrinsic stabilization effects that had defined the PE conformation but that the surrounding effects had to be taken into account in the conformational studies of phospholipid headgroups.

In 1975, the same authors, together with Gresh [34], performed another phospholipid head-conformational study involving the phosphocholine (PC) and phosphoethanolamine (PE) headgroups, the polar groups most often composing the hydrophilic portion [2] of membrane phospholipids. In this study, they investigated solvation effects on the conformations, according to a methodology developed by Pullman et al. [35], based on HF calculations and the PCILO method. The authors concluded that the solvation did in fact induce conformational changes. For the system in an aqueous solution, they found that, for PE, α4 = 240° or 150° and α5 = 60° and, for PC, α4 = 180° and α5 = 300°.

In 1997, Landin, Pascher and Cremer performed a study similar to that performed by Pullman et al. (1975), entitled: “Effect of a Polar Environment on the Conformation of Phospholipid Head Groups Analyzed with the Onsager Continuum Solvation Model” [36]. In this study, using HF methodology and different basis sets, through geometry-optimization calculations they obtained different conformations for the PE and PC systems when isolated and in aqueous solution, starting from the geometric data obtained from the crystallography study. The authors found, similar to Pullman et al. [12], cyclic conformations for the isolated systems (PE: α2 = 274°, α3 = 295°, α4 = 266° and α5 = 75°, PC: α2 = 280°, α3 = 259°, α4 = 242° and α5 = 64°), which became extended forms when in a solvent with a high dielectric constant such as water (PE: α2 = 292°, α3 = 284°, α4 = 142° and α5 = 67°). The cyclic and extended terminologies referred to conformations in which were present or absent, respectively, intramolecular hydrogen bonds between the nonesterified oxygen atoms and the hydrogen atoms of the choline methyl groups (see Fig. 1).

In 1999, Li and Lagowski [37] obtained conformations for the isolated systems glycerophosphorylethanolamine (GPE, α2 = 249°, α3 = 49°, α4 = 260° and α5 = 70°) and glycerophosphorylcholine (GPC, α2 = 67°, α3 = 55°, α4 = 127° and α5 = 292°). As in the other studies mentioned, they used HF/3-21G(d) methodology and X-ray geometric data to build the starting structures.

In 2005, Mrázkova et al. published an interesting theoretical (MD) and experimental study [38]. They reported experimental data from infrared spectroscopy, explaining how hydration was able to induce structural and vibrational changes on the methylphosphocholine molecule (MePC). They concluded that this molecule exhibits a cyclic conformation in the gas phase which tends to become extended under hydration, in agreement with the Landin et al. study [36]. The comparison of the geometric parameters obtained for the most stable conformation in the gas phase and those obtained for the same system (MePC) in a cluster of 48 water molecules indicated that the main structural differences lay in the dihedral angles α4 and α5.

Recently, in 2008, Krishnamurty et al. published the first study, to the best of our knowledge, devoted to the conformational investigation of an entire phospholipid molecule (dimyristoyl phosphatidylcholine, DMPC) [39]. In this study, the authors used density functional theory (DFT) and also structural data from crystallography and NMR in the liquid-crystalline phase to obtain the starting conformations for this system in the gas-phase studies. They performed a study based on the different combinations of the parts of this molecule, namely, the head, neck and body, and tested nearly 200 different starting structures. However, the authors used only two different conformations for the head part, denoted H1 and H2 (H1: α2 = 85°, α3 = 66°, α4 = 121° and α5 = 290°, H2: α2 = 178°, α3 = 45°, α4 = 49° and α5 = 70°). Among all possible combinations, they determined 14 minimum-energy conformations, differing from each other by 1.00 kcal/mol at the most. In this set, both types of heads considered were present.

Therefore, considering the previously discussed theoretical work devoted to the study of the structural features of the phospholipids which compose phospholipid bilayers, we note that much information has been obtained about this system but that in almost all cases the starting geometries were obtained from experiments and only a small part of the conformational space available was investigated. In this work, we attempted to perform a more detailed study to assure a better understanding of these individual units. Such an understanding, therefore, must be the starting point for any deeper discussion regarding phospholipid arrangements.

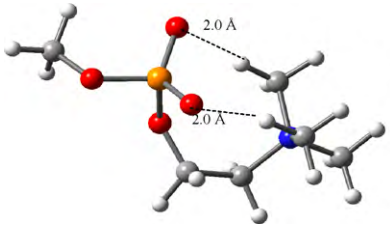

angle/°	(a)	(b)
α3	259	247
α4	242	249

Fig. 2. The starting structure used in the scanning procedure for the angles α3 and α4. The data in column (a) refers to the geometric values of Landin et al. [36], and the data in column (b) refers to this study.

2. Methodology

To obtain the most stable solvated MePC conformations, the quantum-mechanical calculations were performed in different frameworks. The system was first described in the gas phase and then in an aqueous solution, using two, different approaches, as detailed below. All the calculations were performed at the B3LYP/6-31G(d,p) level [40], except when stated otherwise. The calculations were performed with the Jaguar 7.5 [41] and Gaussian03 [42] computational codes. The former uses a pseudospectral methodology to solve the matricial equations, which drastically reduces the computational time, and in the second a version of PCM code is implemented. The solvation energies take into account both the electrostatic and nonelectrostatic components. Frequency calculations were performed for all the conformations, not only to characterize them as stationary minima on the MePC potential-energy surface but also to compute the Boltzmann distribution properly for the system in thermodynamic equilibrium at room temperature and pressure.

2.1. Isolated system

The potential energy surfaces were obtained from a relaxed scan on the dihedral angles α1 (H–C1–O2–P), α2 (C1–O2–P–O3), α3 (O2–P–O3–C4) and α4 (P–O3–C4–C5) (Fig. 1). The variations of α1, α2, α3 and α4 describe rotations around the ∼C1–O2∼, ∼O2–P∼, ∼P–O3∼ and ∼O3–C4∼ bonds, respectively. This detailed scanning was necessary to identify the stable orientations for the molecule, which are very difficult to determine by a simple visual inspection because, in this case, the rotated bonds can change the relative orientation of up to nine lone pairs of electrons (considering all the oxygen atoms). In each calculation, the energy of the system was minimized while the geometric parameters were optimized, except for the dihedral pair of the scanning. Two different conformational maps were obtained when the geometric parameters were split into two sets. The first set encompassed the α3 and α4 variations because they change the energy of the system the most (their modification changes the mutual orientation of the atoms with a formal charge). The starting structure employed to generate the conformational map was obtained from the geometric optimization at the B3LYP/6-31G(d,p) level of the PCgasHF6+ structure reported by Landin et al. [36] (Fig. 2).

The dihedral angles α3 and α4 were scanned in 12 steps of 30° each, generating 144 energy values. These were employed to build a conformational map, through interpolation, using the Radial Basis Function method. Four different regions of stability were found in this map. The values of α3 and α4 that defined them were adjusted in the starting structure, which was fully optimized in the four different ulterior calculations. Two structures converged to the same optimized geometry and the procedure ended with three different conformations. For each conformation, α3 and α4 were kept frozen, and new conformational maps were obtained in the same way but this time scanning on the α1 and α2 angles. Because there were three starting structures, three conformational maps were built. Sampling was performed on these maps and six conformations were found to be stable. Finally, three different values for α5 were investigated (60°, 180° and 300°) for these six stable conformations in calculations where α1, α2, α3, α4 and α5 were kept frozen while all the other geometric parameters were optimized. Eighteen final conformations were then considered in the geometric optimizations, of which only 13 were found to be stationary points.

2.2. Solvated system in an aqueous solution

The solvent effects were introduced using the integral equation formalism [43] (IEFPCM) of the polarizable continuum model [44]. In this approach, the solute is immersed in a cavity opened in the dielectric and the interlocking spheres, centered on the solute atoms or the groups of atoms defining its shape. The radii adopted for these spheres [45] were $\sim CH_3$ = 2.40 Å, $\sim CH_2$ = 2.28 Å, O = 1.82 Å, P = 2.16 Å and N = 1.86 Å, where an alpha factor of 1.2 was assumed. In this approach, an electronic density is calculated for the solute, which takes into account the solvent presence as charge points located on the cavity surface. Once electrostatic effects dominate the interaction between the methylphosphocholine and the water, this model is supposed to properly describe the system in aqueous solution after thermodynamic equilibrium is reached. Although no explicit water molecules were introduced, the water solvent description in the PCM model was able to account for hydrogen-bond-like interactions at a sufficient extension once the decomposition-energy studies for these have shown that the major component (≈65%) has an electrostatic nature [46,47]. This proportion is likely increased in the case of a very polar solute such as MePC when immersed in a solvent with a high dielectric constant such as water.

The solvent effects described within IEFPCM (PCM) were introduced in two different approaches: *Approach 1*: PCM single-point energy evaluations were performed on the starting and final conformations found to be stable for the isolated system after the α5 scanning procedure was completed in the gas phase. This description is useful for quantifying the effects of the solvent alone on the energy and was also extended to the conformations found to be unstable in the gas phase. The latter refers to the starting geometries with values of α5 that "open" the system. Such conformations were considered by allowing competition between the intramolecular and intermolecular (solute-solvent) interactions; *Approach 2*: PCM-optimized geometry calculations were performed for the starting and final conformations found to be stable for the isolated system after the α5 scanning procedure was completed in the gas phase. This description is useful for quantifying the solvent effects on the geometry of the system. In contrast to Approach 1, this approach was able to quantify the degree to which intermolecular interactions affected the final geometries obtained.

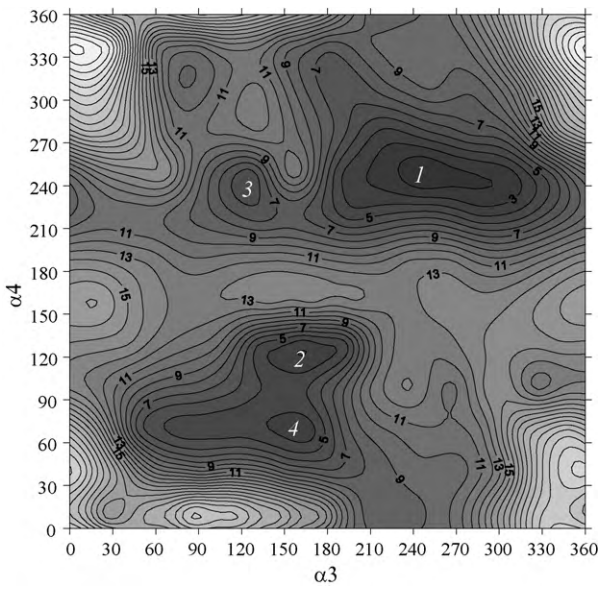

Fig. 3. Relaxed conformational map for MePC as an isolated system, obtained from the interpolation of 144 energy values calculated at the B3LYP/6-31G(d,p) level. Relative energy values are in kcal/mol.

3. Results and discussion

3.1. Isolated system

The conformational map presented in Fig. 3 shows how the energy of MePC was affected by the α3 and α4 dihedral angle variations. Three different conformers were found after sampling in the four minimum-energy regions (regions ***1***, ***2***, ***3*** and ***4***) was performed through geometry-optimization calculations (Table 1) because two geometry-optimization calculations converged to the same structure.

Table 1 exhibits conformational data before and after the geometric optimization calculations as well as the relative energy values found for each conformer. Each one of the four starting structures used had the following values: α1 = 73°, α2 = 284° and α5 = 64°, the same as the starting structure used to generate the map. The latter was obtained from geometric optimizations at the B3LYP/6-31G(d,p) level of the PCgasHF6+ structure reported by Landin et al. [36] (Fig. 2), with α3 and α4 values adjusted to those defining the minimum-energy regions on the map of Fig. 3.

As can be seen in Table 1, the changes in α3 had a greater influence on α2 than those in α4. This can be inferred by comparing the variations of α4 and α2 in conformer ***2*** and those of α3 and α2 in conformer ***3***. This influence can be explained by the fact that the α3 variations changed the geometric coordinates of the atoms with a formal charge, while the converse was not true for α4.

Each conformer of Table 1 was then used as a starting structure in the calculations of three new maps, this time devoted to investigating how the variations of the α1 and α2 dihedral angles affected the MePC energy. The optimized values for the dihedral angles α3 and α4 reported in Table 1 were kept frozen in all the maps shown in Fig. 4.

Independent of the starting geometry (α3 and α4 values), the same two regions of minimum energy can be identified in all the maps for values of α2 ≈ 90° and 270°. Three values for α1 were identified (α1 ≈ 60°, 180° and 300°) for each α2, which correspond to the equivalent minimum-energy regions. This equivalence is due to the symmetrical nature of the methyl group. The variations in α1 describe the C–H bond rotation, which reproduces the original conformation after any 120° rotation. The previous observations led us to select only six conformations, two from each map (regions ***A*** and ***B***).

Furthermore, the energy barriers for the α3 and α4 variations (see Fig. 3) were about six times higher than those for the α1 and α2 variations, which is in agreement with the initial assumption that the variations of the values in the first pair had a higher influence on the MePC energy.

Table 1
Dihedral angles, relative internal and standard Gibbs free energies for conformers found to be stable for the isolated MePC at the B3LYP/6-31G(d,p) level, in degrees and kcal/mol, respectively. Values in parentheses refer to the starting structure.

Conformer	α1	α2	α3	α4	α5	$\Delta U^{\circ}_{T=0\,K}$	$\Delta G^{\circ}_{T=298\,K}$
1	73(73)	285(284)	247(250)	249(250)	64(64)	0[a]	0
2[b]	73(73)	285(284)	158(160)	49(120)	64(64)	1.36	1.51
3	53(73)	203(284)	201(120)	239(240)	64(64)	3.04	2.06

[a] Absolute values for conformer ***1*** are $U^{\circ}_{T=0\,K} = -935.325471$ a.u. and $G^{\circ}_{T=298\,K} = -935.125568$ a.u.
[b] Conformers ***2*** and ***4*** converged to the same geometries during the calculations.

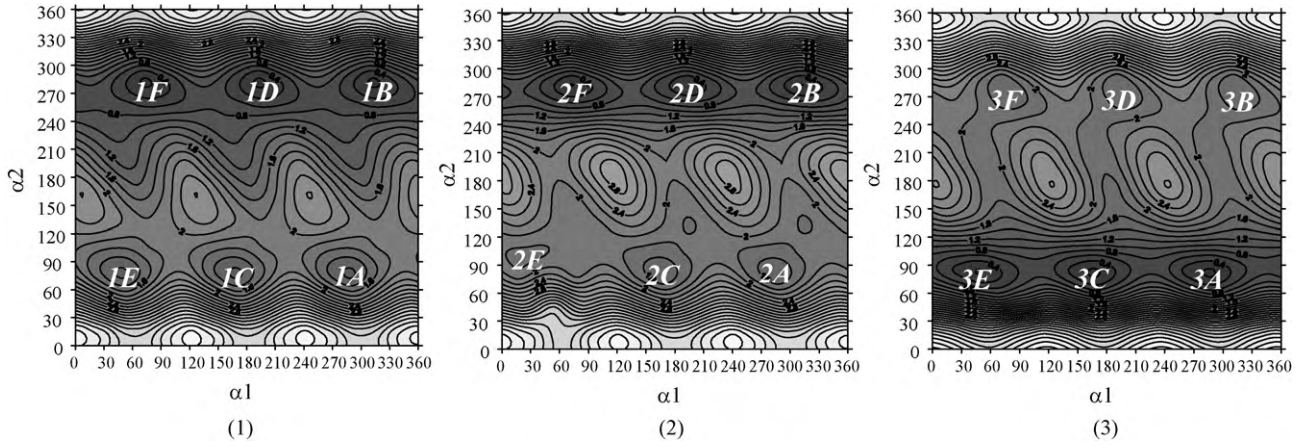

Fig. 4. Relaxed conformational maps (1), (2) and (3), obtained from the starting structures with the same numbering scheme, at the B3LYP/6-31G(d,p) level, obtained from the interpolation of 144 energy values. The relative energy values are in kcal/mol.

Table 2
Geometric parameters α1, α2, α3 and α4 for the MePC conformers as an isolated system. The dihedral angles are in degrees and the relative energies are in kcal/mol, at the B3LYP/6-31G(d,p) level.

Conformer		α1	α2	α3	α4	α5	$\Delta U^{\circ}_{T=0\,K}$	$\Delta G^{\circ}_{T=298\,K}$
Map (1)	***A***	288(73)	72(285)	241(247)	250(249)	65(64)	0.52	0.62
	B	313(73)	285(285)	241(247)	250(249)	65(64)	0[a]	0
Map (2)	***A***	283(73)	77(285)	155(158)	49(49)	65(64)	2.43	2.46
	B	312(73)	285(285)	155(158)	49(49)	65(64)	1.31	1.47
Map (3)	***A***	286(53)	78(203)	199(201)	238(239)	64(64)	1.18	0.86
	B	314(53)	282(203)	199(201)	238(239)	64(64)	2.65	2.21

Absolute values for the conformer ***1B*** are $U^{\circ}_{T=0\,K}$ = −935.325412 a.u. and $G^{\circ}_{T=298\,K}$ = −935.125556 a.u.

Sampling in regions ***A*** and ***B*** was performed through the six geometry-optimization calculations, which considered two different starting structures for each map (each structure corresponding to the geometric parameters defined by the respective minimum-energy region). The results obtained after this step are summarized in Table 2.

In regions ***A*** and ***B***, the stability ordering was found to be: ***1B*** > ***1A*** > ***3A*** > ***2B*** > ***3B*** ≈ ***2A***. The corresponding Boltzmann populations for these conformers were 59, 20, 14, 5, 1 and 1%, respectively. It is important to note that sampling should be performed in all the regions of the map in Fig. 3, even if they appear to be unpopulated at these conditions. This is necessary because other dihedral angles (α1 and α2), once changed, can bring additional stability to the system. Otherwise, relevant conformers may be lost (see conformer ***3A*** in Table 2).

For each of these six conformers, three different values of α5 were investigated. The relative energies of the whole set of conformers are better compared in Fig. 5, below.

As can be seen here, α5 = 60° provided in all cases the most stable conformations followed by α5 = 300°. In both cases, a hydrogen-bond-like interaction was established between the hydrogen atoms of the choline methyl groups and the nonesterified oxygen atoms, as can be visualized in Fig. 6.

All 18 conformers were taken as starting geometries in the completely optimized geometry calculations, generating 13 final conformations, because some of them, namely ***2A***_180, ***2B***_180, ***3A***_180, ***3A***_300 and ***3B***_300 converged to others: ***2A***_300, ***2B***_300, ***1A***_180, ***1A***_300 and ***1B***_300, respectively. This final set of conformers is reported in Table 3, where the dihedral angle range was changed from 0 to 360°, and from −180 to +180°, to facilitate the identification of mirror images between the conformers.

As shown in Table 3, the most abundant conformers of MePC as an isolated system ($p_i \geq 2\%$) were a set of enantiomers because the ***1A***_60 and ***2B***_300 conformers and the ***1B***_60 and ***2A***_300 conformers presented the same values of geometric parameters and energies and, consequently, the same relative abundance. Fig. 6 displays these conformers and illustrates their enantiomeric character with horizontal lines that represent mirrors. The charges on the H, O and N atoms, obtained from the Merz–Kollman–Singh scheme [48], are reported and, where not represented, these values are the same as for the conformer 1A_60.

In the description adopted, all the conformers with α5 = 180° as starting values converged to a value of around 120° for this parameter. This final value allows a closer approximation between the nonesterified oxygen atoms and the hydrogen atoms of the same choline methyl group. The atomic distances between these oxygen and hydrogen atoms (of the same methyl group) changed from approximately 4.2 Å (α5 = 180°) to 2.1 Å (α5 = 120°), enhancing system stabilization.

To evaluate how the size of the basis set and the density of the integration grid of the exchange and correlation functionals affected the geometric and energetic data obtained from the last procedure mentioned (Table 3), we took all the conformers generated from the variation on α5 as the starting geometries for new complete optimized geometry calculations. The new calculation set was performed in two steps: (1) all 18 conformers were reoptimized at the B3LYP/6-311++G(d,p) level and (2) the set of the 13 conformers listed in Table 3 was reoptimized using a tighter grid [41] for the numeric integration of the exchange and correlation functionals at the B3LYP/6-31G(d,p) level. In absolutely all cases, no relevant differences were found for the most stable conformers.

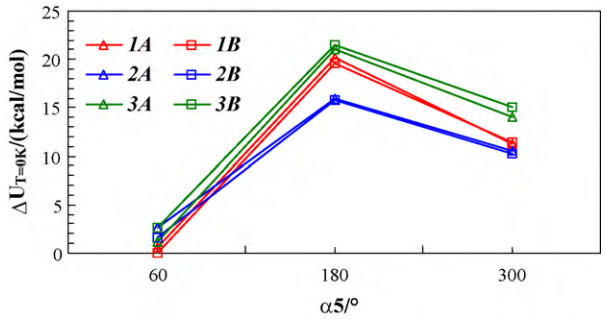

Fig. 5. Relative electronic energies of 18 conformers for three different possible values for α5. In all these calculations, α1, α2, α3 and α4 were frozen at the optimized values reported in Table 2.

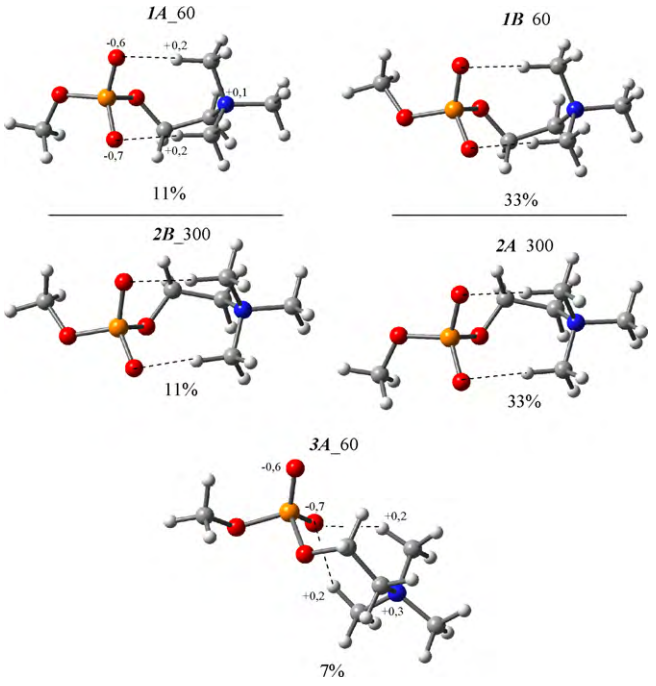

Fig. 6. A set of conformers with abundance ≥2% for MePC in the standard conditions (assumed here as 1 bar and 298.15 K) as an isolated system. All the represented hydrogen bonds have a length of ≈2.0 Å.

Table 3
The geometric and energetic data for the final 13 conformers of MePC found to be thermodynamically stable in the gas phase. The dihedral angles are in degrees, the relative standard Gibbs free energies are in kcal/mol and the Boltzmann populations (p_i) are percentages.

Conformer[a]	α1	α2	α3	α4	α5	$\Delta U^\circ_{T=0\,K}$	$\Delta G^\circ_{T=298\,K}$	p_i (%)
1A_60	−73	73	−125	−108	66	0.52	0.66	11
1A_180	−73	73	−169	−70	123	4.79	4.78	0
1A_300	−73	73	−126	−70	−52	3.43	3.07	0
1B_60	−49	−77	−112	−111	64	−0.01	0.01	33
1B_180	−49	−77	−57	−70	127	7.21	6.51	0
1B_300	−49	−77	−92	−70	−46	2.43	2.25	1
2A_60	−75	76	151	49	65	2.46	2.54	0
2A_300	−75	76	113	111	−64	0[b]	0	34
2B_60	−49	−73	155	49	65	1.34	1.57	2
2B_300	−49	−73	125	108	−66	0.52	0.67	11
3A_60	−74	76	−167	−122	65	1.20	0.92	7
3B_60	−47	−77	−155	−121	63	2.68	2.28	1
3B_180	−47	−77	−166	−71	123	5.34	5.17	0

[a] The notation used in the conformer identification refers to α3 and α4 (***1***, ***2*** and ***3***), α1 and α2 (***A*** and ***B***) and to the starting value for α5 in the geometry-optimization calculations (60, 180 and 300°).
[b] Absolute values for the conformer ***2A***_300 are $U^\circ_{T=0\,K}$ = −935.325456 a.u. and $G^\circ_{T=298\,K}$ = −935.125647 a.u.

3.2. Solvated system

3.2.1. Approach 1

All 13 conformers obtained as stable conformations in the gas phase were solvated in PCM through single-point energy calculations. Additionally, the other six conformations were considered, all of them with α5 set at 180° (the starting conformations reported in Fig. 5). This new set was introduced to account for the competition between the intermolecular (solute–solvent) and the intramolecular hydrogen-bond-like interactions present in the extended (α5 = 180°) and the cyclic (α5 = 60° and 300°) conformations, respectively, in our notation. The results are summarized in Table 4 below.

Here, we can see that the conformations with α5 set at 180° were not abundant in PCM, at least under the single-point approximation. Furthermore, the Boltzmann population values were changed a great deal compared to those calculated for the isolated system, indicating the influence of solute-solvent interactions. These results prompted us to consider such interactions at a deeper level and also to investigate their influence on the geometric parameters of the system.

Table 4
Single-point calculations for the MePC conformers in PCM. $\Delta G^{elec}_{T=0\,K}$ and $\Delta G^{non\text{-}elec}$ are relative values for the electrostatic and the nonelectrostatic components of the final solvation energy ($\Delta G^\circ_{T=298\,K}$), in kcal/mol. Boltzmann populations are percentages.

Conformer	$\Delta G^{elec}_{T=0\,K}$	$\Delta G^{non\text{-}elec}$	$\Delta G^\circ_{T=298\,K}$	p_i (%)
1A_60	−0.06	−0.08	0.64	15
1A_180	4.14	−0.20	4.40	0
1A_180$_{imp}$	3.89	0.60	4.24	0
1A_300	1.82	0.10	2.09	1
1B_60	0.18	−0.11	0.90	9
1B_180	4.05	0.16	3.75	0
1B_180i$_{imp}$	4.19	0.48	5.77	0
1B_300	1.73	0.01	2.36	1
2A_60	3.38	0.03	4.02	0
2A_180$_{imp}$	6.28	0.34	6.03	0
2A_300	0.24	−0.11	0.91	9
2B_60	2.64	−0.08	3.51	0
2B_180$_{imp}$	5.77	0.40	5.81	0
2B_300	−0.03	−0.08	0.66	14
3A_60	0[a]	0	0	43
3A_180$_{imp}$	5.02	0.53	5.05	0
3B_60	0.72	0.15	1.01	8
3B_180	4.30	−0.18	4.60	0
3B_180$_{imp}$	5.02	0.53	5.28	0

[a] The absolute values for the conformer ***3A***_60 are $G^{elec}_{T=0\,K}$ = −935.367729 a.u., $G^{non\text{-}elec}$ = 3.08 kcal/mol and $G^\circ_{T=298\,K}$ = −935.164126 a.u.

3.2.2. Approach 2

All 19 conformers of Approach 1 were solvated in PCM but this time in calculations where all the geometric parameters were optimized (the details of the geometric parameters are provided in Supporting Information). The geometric data were better than those in the gas phase in Fig. 7. Fig. 8 compares the relative abundance values obtained for all the conformations in each description.

In Fig. 7, the main dihedral angles of MePC are reported for the isolated system and the system in PCM (as in Approach 2). Because the solute–solvent interaction affects each dihedral differently, we will outline the main observations separately. For α1, there was no relevant modification, not only with respect to the medium value (the gas phase or aqueous solution) but also for the final value: all the conformers present α1 ≈ −60°. Similarly to α1, α2 did not change very much from the gas phase to solution, but two possible values were found for all the considered conformers: −60° and 60°. Interestingly, all the values found in PCM were smaller in the module than in the gas phase. The dihedral angles α3 and α4 were the geometric parameters most sensitive to solvation. This may be related to the fact that their values define a particular orientation of the moieties with a formal charge. As the considered solvent has a high dielectric constant, it would be expected that the solute–solvent interactions help in the MePC stabilization of these moieties. If the solute–solvent interactions favored in the geometries obtained in PCM did not compensate for the intramolecular ones present in the isolated system, no significant geometric modifications would be observed. The conformers that presented the largest variations in α3 and α4 (1B_60 and 2A_300) are mirror images of each other. In the set of conformers studied, except for 1B_180, the value for the dihedral angle α5 was practically independent of the phase (gas or aqueous solution).

The data reported in Table 5 take into account the geometric changes introduced by the presence of the solvent in the final relative abundances found for all the conformers described by Approach 2.

The Boltzmann population values for all the descriptions of the MePC conformers as isolated and solvated systems in both the approaches for the solvated system are compared in Fig. 8.

The Boltzmann population of each conformer was drastically affected by the solvent presence as well as by the way it was introduced. Assuming that Approach 2 is a description closer to the physical system, surprisingly, the relative abundance obtained for Approach 2 was better reproduced by the isolated system (see the 1B_60 and 2A_300 conformers) rather than by Approach 1. However, a very abundant conformer was lost (1B_300) if the

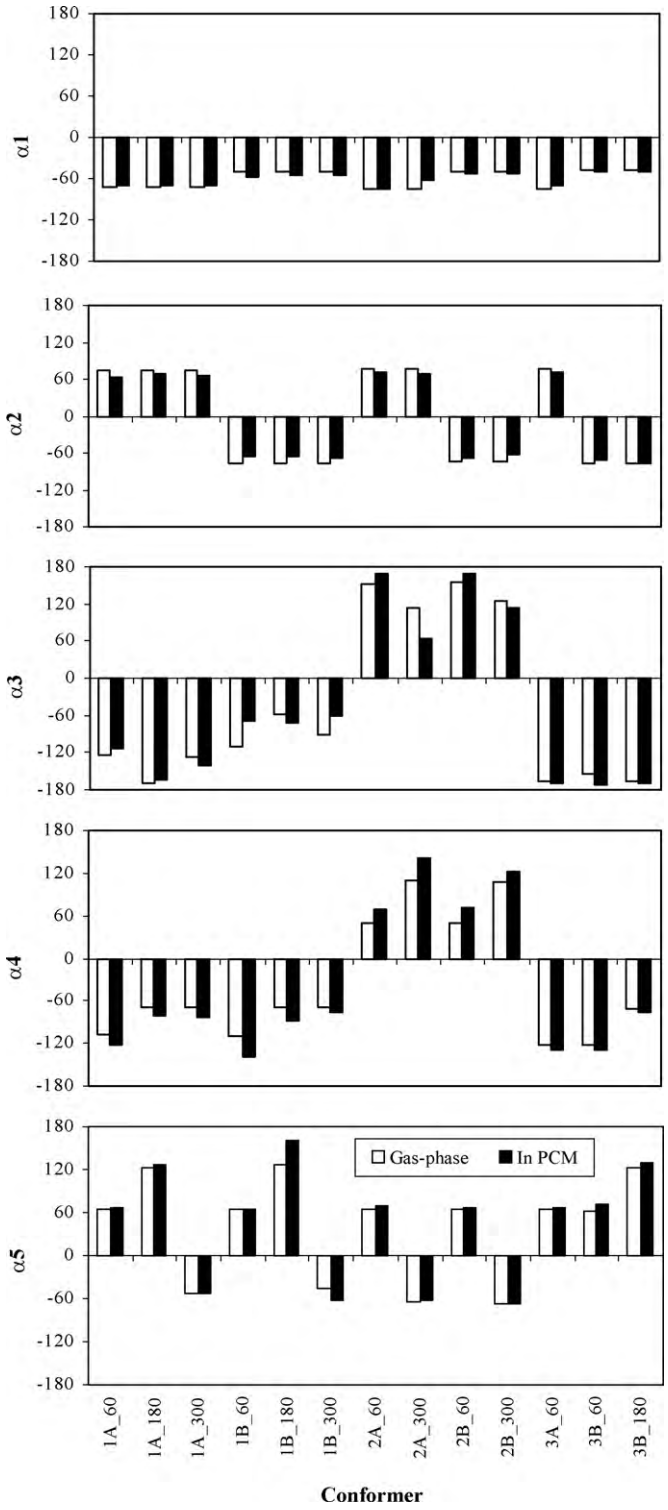

Fig. 7. The geometric values of the main dihedral angles of MePC as an isolated system and solvated by PCM.

solute–solvent interaction was not extended to the geometry (Approach 2). Likely due to the geometric modifications needed to maximize the solute-solvent interactions allowed in Approach 2, Approach 1 was not a good description, providing results worse than those of the gas-phase approximation. Fig. 9 shows the conformers obtained for MePC as an isolated system and in an aqueous solution and their respective Boltzmann populations. The charges on the H, O and N atoms, obtained from the Merz–Kollman–Singh

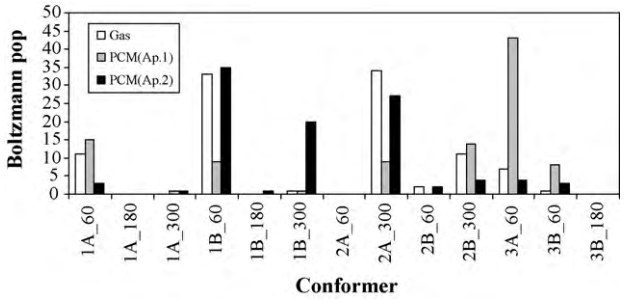

Fig. 8. Boltzmann population values for the conformers in the gas phase and in PCM in single-point energy (Approach 1) and geometry-optimization (Approach 2) calculations.

Scheme [48], are reported and, where not represented, these values are the same as the conformer 1A_60 in both phases.

In general, the intramolecular hydrogen-bond distances observed in the conformers in the gas phase were enlarged in PCM, displaying a type of competition between the stabilization effects originating from the intermolecular or intramolecular interactions. In fact, it seems to be the main role of the solvent in these systems to weaken or even to suppress the intramolecular hydrogen bonds (see 1B_300).

3.3. Comparison with experimental data

Taking into account the geometric data available in the literature for the different phosphocholine derivatives in the crystalline and the liquid-crystalline phases, some comparisons are possible.

In the following figures, two sets of data are reported, where the experimental values of α2, α3, α4 and α5 are exhibited for the systems in different phases and then finally compared to those found in this study. First, in Fig. 10, the experimental data for some MePC derivatives are reported and compared with the systems in two different phases. The derivatives in the crystalline phase are: 1,2-dimyristoyl-*sn*-glycero-3-phosphocholine dihydrate (DMPC), 1-palmitoyl-*sn*-glycero-3-phosphocholine monohydrate (PPC), 1-hexadecyl-*sn*-glycero-3-phosphocholine (HPC) and *sn*-glycero-3-phosphocholine (GPC) [49]. The numbers 1, 2, 3, 4 and 5 for the

Table 5
The completely optimized geometry calculations for the MePC conformers in PCM. $\Delta G^{elec}_{T=0\,K}$ and $\Delta G^{non\text{-}elec}$ are the relative values for the electrostatic and non-electrostatic components of the final solvation energy ($\Delta G^{\circ}_{T=298\,K}$) in kcal/mol. The Boltzmann populations are percentages.

Conformer	$\Delta G^{elec}_{T=0\,K}$	$\Delta G^{non\text{-}ele}$	$\Delta G^{\circ}_{T=298\,K}$	p_i (%)
1A_60	0.36	0.08	1.48	3
1A_180	4.68	−0.17	4.07	0
1A_180$_{imp}$	3.87	−0.10	2.40	1
1A_300	1.36	−0.04	2.10	1
1B_60	0[a]	0	0	35
1B_180	2.89	−0.01	2.26	1
1B_180$_{imp}$	2.50	−0.13	3.18	0
1B_300	0.67	−0.12	0.33	20
2A_60	1.30	0.03	5.79	0
2A_180$_{imp}$	3.69	0.10	4.40	0
2A_300	−0.03	−0.04	0.15	27
2B_60	1.38	−0.11	1.80	2
2B_180$_{imp}$	3.83	−0.09	2.79	0
2B_300	0.34	0.06	1.32	4
3A_60	0.71	0.00	1.31	4
3A_180$_{imp}$	3.87	−0.07	3.31	0
3B_60	0.55	0.06	1.49	3
3B_180	4.90	−0.12	4.73	0
3B_180$_{imp}$	3.97	−0.06	5.27	0

[a] The absolute values for the conformer 1B_60 are $G^{elec}_{T=0\,K}$ = −935.373809 a.u., $G^{non\text{-}elec}$ = 3.86 kcal/mol and $G^{\circ}_{T=298\,K}$ = −935.170661 a.u.

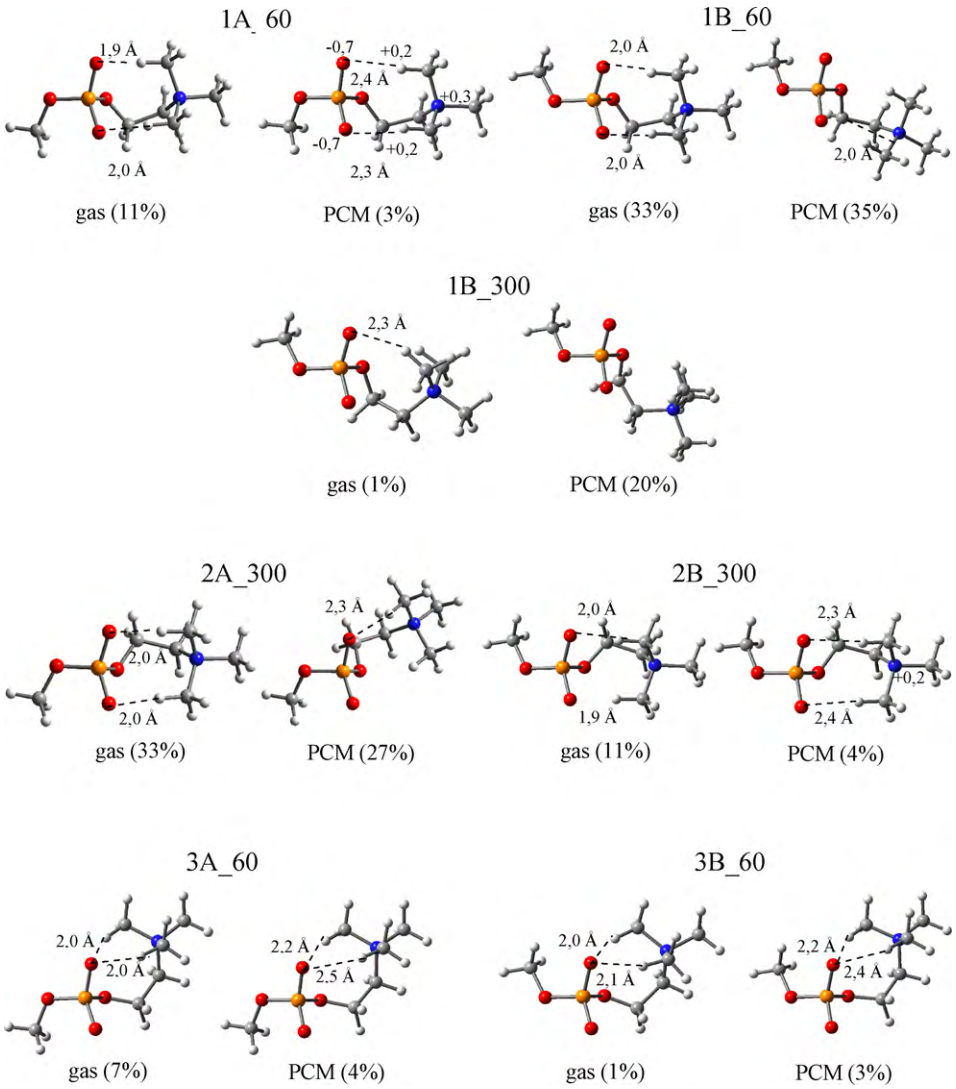

Fig. 9. The MePC conformers in the gas phase and in PCM. The values in parentheses are the Boltzmann populations for the system at standard conditions.

1,2-dipalmitoyl-*sn*-glycero-3-phosphocholine (DPPC) in the liquid-crystalline phase refer to the possible [50] conformations found experimentally.

Comparing both sets of data, we can see that the main difference occurs with the α5 values, which in the crystalline phase is about 60° while in the liquid-crystalline phase can be 60° or −60° (300°). In both phases, the most common values found for α3 are 60° and −60°, while for α4 they are 150° and −150°. Independent of the phase where the phospholipid is studied, α3 and α4 maintain their mirror-image pattern. Additionally, it is important to note that the values of these dihedral angles are little affected by the hydrophobic segment because all the derivatives studied presented approximately the same values.

In Fig. 11, the geometric values of α2, α3, α4 and α5 are reported for the systems investigated in this study and also for other conformations studied by Landin et al. [36] (PCgasHF6+, PCsolextHF6+ and PCsolcycHF6+), Pullman [34] (GPC) and Krishnamurty et al. [39] (DMPC H1 and 2). PCgasHF6+ is the most abundant conformation in the gas phase [36], GPC is a phosphocholine prototype larger than MePC [35b] and DMPC (H1/H2) are two conformations found abundant as a complete phospholipid unit. The conformations are identified by the nomenclature used in Approach 2.

From Fig. 11, it can be seen that the other studies did not find any mirror-image patterns among the set of selected conformers, independent of the phase. However, in this study, the two most abundant sets of conformations (red and orange) presented this characteristic (the chiral behavior is reported as solid and slashed columns). The values found for these in Approach 2: 1B_60 (2A_300) and 1A_60 (2B_300) are in very good agreement with those found experimentally for the phospholipid membranes of the different derivatives of MePC and, together with 1B_300, are the five conformers comprising approximately 90% of the MePC occurring in an aqueous solution.

3.4. Analytical expressions for potential curves for α3 and α4

This work provided a conformational landscape in dihedral space at a quantum-mechanical level that includes (partially) electronic correlation effects. The dihedral parameters α3 and α4 were shown to be those for which variations most affect the energy of the system. Therefore, in the next paragraphs we present two potential curves obtained from fittings of the variations observed in the quantum-mechanical energies due to α3 and α4 variations in terms of cosine functions and Fourier series. These fittings were obtained for the system in the gas phase, and, although they are not the parameterizations of this dihedral space that should be directly included in a force field (because to do that it would be necessary to choose the force field and their respective topology and parameter

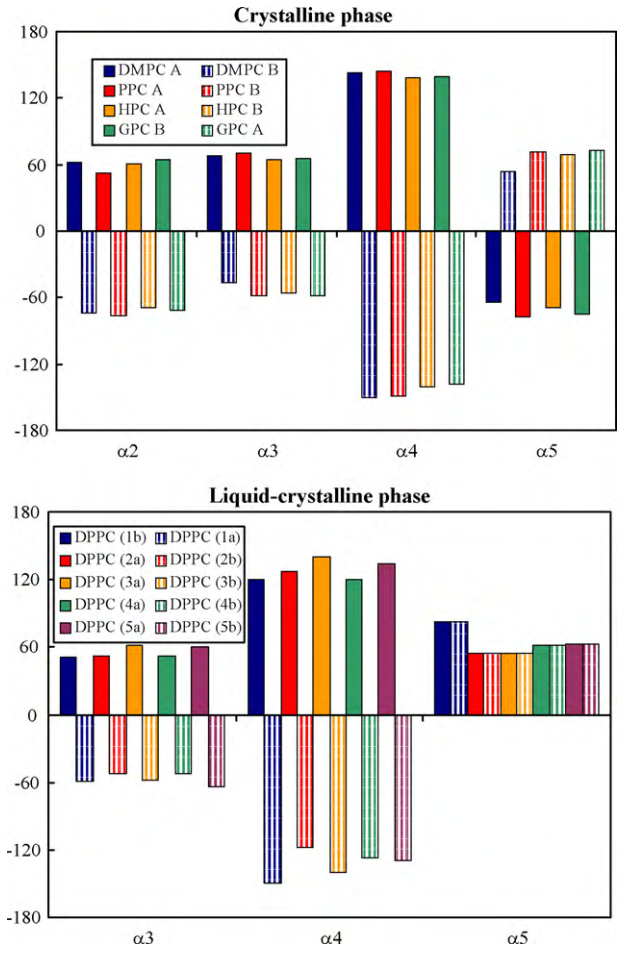

Fig. 10. Experimental (crystalline) and estimated (liquid-crystalline) values for α2, α3, α4 and α5 of MePC derivatives in two distinct phases. The A/B (or a/b) notation refers to the corresponding pair of mirror images.

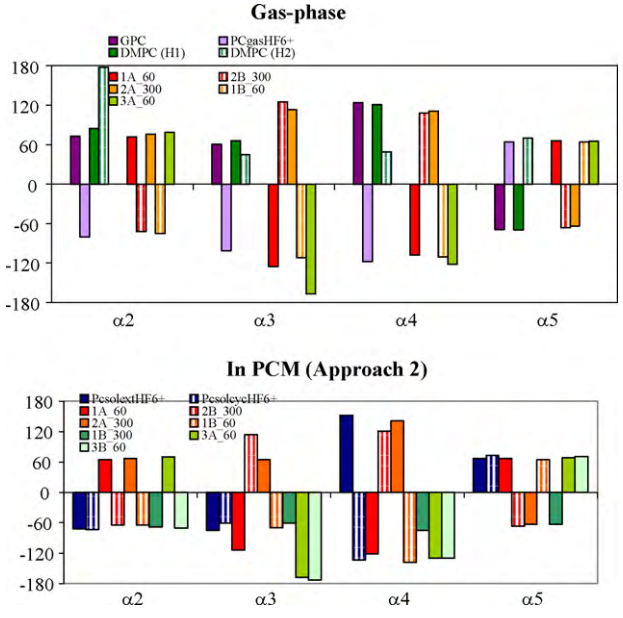

Fig. 11. The theoretical values of the α2, α3, α4 and α5 dihedral angles of MePC found in this study and in the literature.

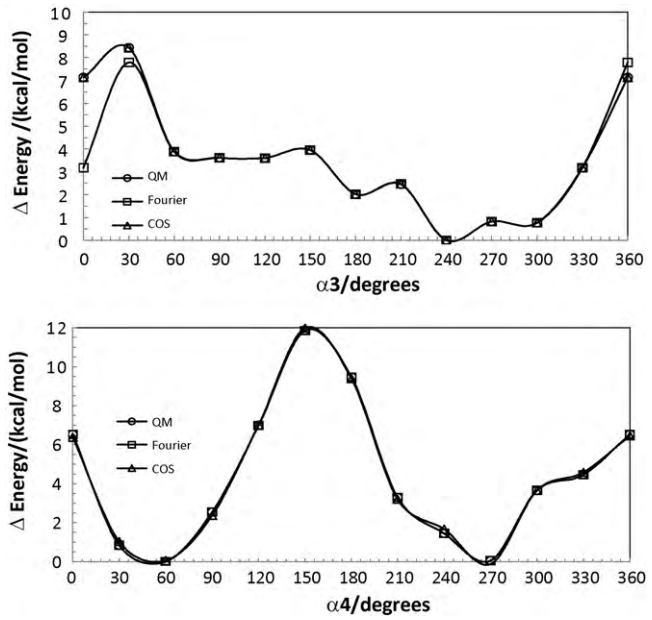

Fig. 12. Potential curves obtained for α3 and α4 from the map of Fig. 3. Two fittings (cosines and Fourier series) are reported for the original quantum-mechanical potential curve; their coefficients are presented in Tables 6 and 7. The absolute values for the quantum-mechanical potential curves are −935.325001 a.u. and −935.322362 a.u. for the scan in α3 and α4 dihedral angles, respectively.

files), they offer an analytical expression with which to begin such a procedure. The geometries of the conformers used can be found in Supplementary Data, as well as the corresponding energy values.

In this procedure, for the potential curve showing how the energy of the system changes with α3, the α4 values for each starting geometry were read from the map of Fig. 3 as those that minimized the energy for the corresponding α3 value. The geometry of the whole system was optimized in two steps during the scan in α3: in the first, both α3 and α4 values were frozen and the final geometry was used as the starting point of the successive step. In the last step, only α3 was kept frozen during the geometric optimization; the equivalent procedure was repeated for α4.

The final potential curves for αx, x = 3 or 4, are reported in Fig. 12, and their corresponding mathematical expressions are given below and in Tables 6 and 7:

$$E(ax) = \sum_{i=1}^{6} A_i \cos(B_i \alpha x) + C_i \mathrm{sen}(B_i \alpha x), \text{ for the Fourier series and}$$

$$E(\alpha x) = \sum_{i=1}^{12} A_i \cos(iB\alpha x), \text{ for the cosine functions, where } B = 2.069$$

Table 6
Coefficients for the Fourier series fitting the quantum-mechanical potential-energy curves (at B3LYP/6-31G(d,p) level) obtained for α3 and α4 from the conformational map of Fig. 3.

i	α3			α4		
	A_i	B_i	C_i	A_i	B_i	C_i
0	2.918	0	0	4.260	0	0
1	0.383	0.019	2.106	−2.306	0.017	1.098
2	0.790	0.038	1.003	2.927	0.035	−3.084
3	0.024	0.057	0.888	0.307	0.052	0.407
4	−0.613	0.076	0.507	0.388	0.070	−0.432
5	−0.321	0.095	0.716	0.534	0.087	0.558
6	0	0	0	0.420	0.105	0.648

Table 7
Coefficients for the cosine series fitting the quantum-mechanical potential-energy curves (at B3LYP/6-31G(d,p) level) obtained for α3 and α4 from the conformational map of Fig. 3.

i	α3 A_i	α4 A_i
0	2.544	5.190
1	−2.346	−4.152
2	0.630	−0.787
3	−0.534	0.618
4	0.648	0.386
5	−0.116	0.715
6	−0.163	0.526
7	2.322	3.405
8	2.590	−1.398
9	2.828	−1.222
10	0.171	3.095
11	0.027	0
12	−0.166	0

It is worth stressing that in both cases the number of terms proposed are higher than that commonly used in a force-field parameterization, but these expressions are only a fitting of the raw relative energy values obtained from the quantum-mechanical calculations. They are not intended to represent the corresponding torsional dependence of any force field, which should be still obtained after the force field is chosen.

4. Conclusions

A conformational study of MePC was performed through an analysis of changes in the electronic energy of this system with a systematic variation of the five dihedral angles that define the orientation of the MePC main chain. The calculations were performed at the B3LYP/6-31G(d,p) level, in a gas phase and in PCM. The set of conformers found allowed us to conclude that the phospholipid head is a zwitterionic system that occurs in many thermodynamically stable conformations in the gas phase and in the aqueous solution.

According to the results of this study, the geometric parameters α3 and α4 most greatly affected the energy of the system. This is because their variations change both the relative orientations of the lone pairs of the electrons of the oxygen atoms of the main backbone of MePC (the α-chain in phospholipid nomenclature [51]) and the positions of the moieties with formal charge in the molecule, i.e., the nonesterified oxygen atoms.

With respect to the description obtained in the gas phase, the two most important conformations found for the isolated system (***1B***_60 and ***2A***_300) had a relative abundance of 67%. These were also found in Approach 2 (62%) and were very distinct from those in Approach 1, where the solvent effects were constrained to within the energy of the system. In this latter approach, the most abundant conformations found were ***3A***_60 (43%) and ***1A***_60 (15%). The population values obtained from Approach 1 were also very different from those found in the gas phase and in Approach 2.

New conformations, which were somewhat different from those found to be stable in the gas phase, were obtained for the system in an aqueous solution when the solvent effects were considered in the geometry (Approach 2) using the PCM method. The main modifications in the geometry of the system were associated with the α3 and α4 values.

A mirror-image pattern was observed among the most stable conformations in Approach 2, in agreement with the experiments. This suggests that the final set of conformations obtained from the theoretical sampling of MePC PES is able to properly describe the system, without any empirical information.

Acknowledgments

The authors would like to thank the Brazilian agencies CNPq, CAPES and FAPERJ, for the financial support given to this work.

Appendix A. Supplementary data

Supplementary data associated with this article can be found, in the online version, at doi:10.1016/j.jmgm.2010.05.001.

References

[1] S.R. Bolsove, J.S. Hyams, E.A. Shephard, H.A. White, C.G. Wiedemann, Cell Biology, A Short Course, 2nd ed., John Wiley & Sons, 2004.
[2] M.K. Jain, R.C. Vagner, Introduction to Biological Membranes, John Wiley & Sons, 1980.
[3] P. Cerruti, M.S. de Huergo, M. Galvagno, C. Schebor, M.B. Puera, Commercial baker's yeast stability as affected by intracellular content of trehalose, dehydration procedure and the physical properties of external matrices, Appl. Microbiol. Biotechnol. 54 (2000) 575–580.
[4] J.H. Crowe, F. Tablin, W.F. Wolkers, K. Gousset, N.M. Tsvetkova, J. Ricker, Stabilization of membranes in human platelets freeze-dried with trehalose, Chem. Phys. Lipids 122 (2003) 41–52.
[5] G.R. Satpathy, Z. Torok, R. Bali, D.M. Dwyre, E. Little, N.J. Walker, F. Tablin, J.H. Crowe, N.M. Tsvetkova, Loading red blood cells with trehalose: a step towards biostabilization, Cryobiology 49 (2004) 123–136.
[6] L.K. McGinnis, L.B. Zhu, J.A. Lawitts, S. Bhowmick, M. Toner, J.D. Biggers, Mouse sperm desiccated and stored in trehalose medium without freezing, Biol. Reprod. 73 (2005) 627–633.
[7] F.A. Hoekstra, E.A. Golovina, J. Buitink, Mechanisms of plant desiccation tolerance, Trends Plant Sci. 6 (2001) 431–438.
[8] J.H. Crowe, J.F. Carpenter, L.M. Crowe, The role of vitrification in anhydrobiosis, Ann. Rev. Physiol. 60 (1998) 73–103.
[9] J.H. Crowe, L.M. Crowe, Membranes, in: A.C. Leopold (Ed.), Metabolism and Dry Organisms, University Press, Ithaca, 1986 (Chapter 11).
[10] K.L. Koster, Y.P. Lei, M. Anderson, S. Martin, G. Bryant, Effects of vitrified and nonvitrified sugars on phosphatidylcholine fluid-to-gel phase transitions, Biophys. J. 78 (2000) 1932–1946.
[11] E.R. Caffarena, J.R. Grigera, Glass transition in aqueous solutions of glucose. Molecular dynamics simulation, Carbohydr. Res. 300 (1997) 51–57.
[12] E.R. Caffarena, J.R. Grigera, Hydration of glucose in the rubbery and glassy states studied by molecular dynamics simulation, Carbohydr. Res. 315 (1999) 63–69.
[13] C.S. Pereira, P.H. Hünenberger, Interaction of the sugars trehalose, maltose and glucose with a phospholipid bilayer: a comparative molecular dynamics study, J. Phys. Chem. B 110 (2006) 15572–15581.
[14] C.S. Pereira, R.D. Lins, I. Chandrasekhar, L.C.G. Freitas, P.H. Hünenberger, Interaction of the disaccharide trehalose with a phospholipid bilayer: a molecular dynamics study, Biophys. J. 86 (2004) 2273–2285.
[15] A.K. Sum, R. Faller, J.J. de Pablo, Molecular simulation study of phospholipid bilayers and insights of the interactions with disaccharides, Biophys. J. 85 (2004) 2830–2844.
[16] N.M. Tsvetkova, B.L. Phillips, L.M. Croew, J.H. Crowe, S.H. Risbud, Effect of sugars on headgroup mobility in freeze-dried dipalmotiylphosphatidylcholine bilayers: solid-state ^{31}P NMR and FTIR studies, Biophys. J. 75 (1998) 2947–2955.
[17] C.W.B. Lee, J.S. Waugh, R.G. Griffin, Solid-state NMP study of trehalose/1,2-dipalmitoyl-*sn*-phosphatidylcholine interactions, Biochemistry 25 (1986) 3737–3742.
[18] C. Lambruschini, A. Relini, A. Ridi, L. Cordone, A. Gliozzi, Trehalose interacts with phospholipid polar heads in Langmuir monolayers, Langmuir 16 (2000) 5467–5470.
[19] C.S. Pereira, P.H. Hünenberger, The influence of polyhydroxylated compounds on a hydrated phospholipid bilayer: a molecular dynamics study, Mol. Simul. 34 (2008) 403–420.
[20] (a) C.O. da Silva, M.A.C. Nascimento, Ab initio conformational maps for disaccharides in gas phase and aqueous solution, Carbohydr. Res. 339 (2004) 113–122;
(b) C.S. Soares, C.O. Silva, Determinação teórica das conformações mais estáveis da trealose em solução aquosa, Quím. Nova 31 (2008) 280–284;
(c) F. Javaroni, A.B.B. Ferreira, C.O. da Silva, The (alpha-1,6) glycosidic bond of isomaltose: a tricky system for theoretical conformational studies, Carbohydr. Res. 344 (2009) 1235–1247;
(d) C.O. da Silva, B. Mennucci, T. Vreven, Density functional study of the optical rotation of glucose in aqueous solution, J. Org. Chem. 69 (2004) 8161–8164.
[21] K. Thirumoorthy, N. Nandi, D. Vollhardt, O.N. Oliveira, Semiempirical quantum mechanical calculations of dipolar interaction between dipyridamole and dipalmitoyl phosphatidyl choline in Langmuir monolayers, Langmuir 22 (2006) 5398–5402.
[22] Y. Duan, C. Wu, S. Chowdhury, M.C. Lee, G.M. Xiong, W. Zhang, R. Yang, P. Cieplak, R. Luo, T. Lee, J. Caldwell, J.M. Wang, P. Kollman, A point-charge force field for molecular mechanics simulations of proteins based on condensed-phase quantum mechanical calculations, J. Comput. Chem. 24 (2003) 1999–2012.

[23] G.A. Kaminski, R.A. Friesner, J. Tirado-Rives, W.L. Jorgensen, Evaluation and reparametrization of the OPLS-AA force field for proteins via comparison with accurate quantum chemical calculations on peptides, J. Phys. Chem. B 105 (2001) 6474–6487.
[24] S.E. Feller, A.D. MacKerell Jr., An improved empirical potential energy function for molecular simulations of phospholipids, J. Phys. Chem. B 104 (2000) 7510–7515.
[25] S.J. Marrink, A.E. Mark, Molecular view of hexagonal phase formation in phospholipid membranes, Biophys. J. 87 (2004) 3894–3900.
[26] K. Murzyn, W. Zhao, M. Karttunen, M. Kurdziel, T. Rog, Dynamics of water at membrane surfaces: effect of headgroup structure, Biointerphases 1 (2006) 98–105.
[27] T. Rog, K. Murzyn, M. Pasenkiewicz-Gierula, The dynamics of water at the phospholipid bilayer surface: a molecular dynamics simulation study, Chem. Phys. Lett. 352 (2002) 323–327.
[28] J. Chanda, S. Bandyopadhyay, Perturbation of phospholipid bilayer properties by ethanol at a high concentration, Langmuir 22 (2006) 3775–3781.
[29] C.J. Högberg, A.P. Lyubartsev, A molecular dynamics investigation of the influence of hydration and temperature on structural and dynamical properties of a dimyristoylphosphatidylcholine bilayer, J. Phys. Chem. B 110 (2006) 14326–14336.
[30] J. Thaning, C.J. Hoegberg, B. Stevensson, A.P. Lyubartsev, A. Maliniak, Molecular conformations in a phospholipid bilayer extracted from dipolar couplings: a computer simulation study, J. Phys. Chem. B 111 (2007) 13638–13644.
[31] B. Pullman, H. Berthod, Quantum-mechanical studies on conformation of phospholipids—conformational properties of polar head, FEBS Lett. 44 (1974) 266–269.
[32] K.S. Bruzik, J.S. Harwood, Conformational study of phospholipids in crystalline state and hydrated bilayers by C-13 and P-31 CP-MAS NMR, J. Am. Chem. Soc. 119 (1997) 6629–6637.
[33] F. Aussenac, M. Laguerre, J.M. Schmitter, E.J. Dufourc, Detailed structure and dynamics of bicelle phospholipids using selectively deuterated and perdeuterated labels. H-2 NMR and molecular mechanics study, Langmuir 19 (2003) 10468–10479.
[34] B. Pullman, H. Berthod, N. Gresh, Quantum-mechanical studies on conformation of phospholipids—effect of water on conformational properties of polar head, FEBS Lett. 53 (1975) 199–204.
[35] B. Pullman, A. Pullman, Molecular orbital calculations on the conformation of amino acid residues of proteins, Adv. Protein Chem. 28 (1974) 347–526 (and references therein).
[36] J. Landin, I. Pascher, D. Cremer, Effect of a polar environment on the conformation of phospholipid head groups analyzed with the Onsager continuum solvation model, J. Phys. Chem. A 101 (1997) 2996–3004.
[37] W. Li, J.B. Lagowski, Ab initio study of phospholipid headgroups: GPE and GPC, Chem. Phys. Lipids 103 (1999) 137–160.
[38] E. Mrázková, P. Hobza, M. Bohl, D.R. Gauger, W. Pohle, Hydration-induced changes of structure and vibrational frequencies of methylphosphocholine studied as a model of biomembrane lipids, J. Phys. Chem. B 109 (2005) 15126–15134.
[39] S. Krishnamurty, M. Stefanov, T. Mineva, S. Begu, J.M. Devoisselle, A. Goursot, R. Zhu, D.R. Salahub, Density functional theory-based conformational analysis of a phospholipid molecule (dimyristoyl phosphatidylcholine), J. Phys. Chem. B 112 (2008) 13433–13442.
[40] A.D. Becke, Density-functinal thermochemistry. III. The role of exact exchange, J. Chem. Phys. 98 (1993) 5648–5652.
[41] Jaguar, Version 7.5, Schrödinger, LLC, New York, NY, 2008.
[42] M.J. Frisch, et al., Gaussian 03 (Revision C.01), Gaussian Inc., Pittsburg, PA, 2003.
[43] E. Cancés, B. Mennucci, J. Tomasi, A new integral equation formalism for the polarizable continuum model: Theoretical background and applications to isotropic and anisotropic dielectrics, J. Phys. Chem. 107 (1997) 3032–3041.
[44] S. Miertus, E. Scrocco, J. Tomasi, Electrostatic interaction of a solute with a continuum—a direct utilization of ab initio molecular potentials for the prevision of solvent effects, Chem. Phys. 55 (1981) 117–129.
[45] A. Bondi, van der, Waals volumes + radii, J. Phys. Chem. 68 (1964) 441–451.
[46] H. Umeyama, K. Morokuma, The origin of hydrogen bonding. An energy decomposition study, J. Am. Chem. Soc. 99 (1977) 1316–1332.
[47] Y. Mo, J. Gao, S.D. Peyerimhoff, Energy decomposition analysis of intermolecular interactions using a block-localized wave function approach, J. Chem. Phys. 112 (2000) 5530–5538.
[48] J.B. Foresman, Æ. Frisch, Exploring Chemistry with Electronic Structure Methods, 2nd ed., Gaussian, Inc., 1996.
[49] I. Pascher, M. Lundmark, P.G. Nyholm, S. Sundell, Crystal-structures of membrane-lipids, Biochim. Biophys. Acta 1113 (1992) 339–373.
[50] H. Akutsu, T. Nagamori, Conformational analysis of the polar head group in phosphatidylcholine bilayers—a structural-change induced by cations, Biochemistry 30 (1991) 4510–4516.
[51] M. Sundaralingam, Discussion paper: molecular structures and conformations of the phospholipids and sphingomyelins, Ann. N.Y. Acad. Sci. 195 (1972) 324–355.